Available online www.jsaer.com

***Journal of Scientific and Engineering Research*, 2017, 4(6):161-169**

Research Article

ISSN: 2394-2630
CODEN(USA): JSERBR

Porous Media Influence on the Transport Phenomena in the Polymer Electrolyte Membrane Fuel Cell

LARBI Badreddine*, ALIMI Wael, CHOUIKH Ridha, GUIZANI Amenallah

Centre des Recherches et technologies de l'énergie, Laboratoire des procédés thermiques, BP 95, Hammam LIF, 2050, Tunisia

Abstract One of the critical factors which determine the performance of PEMFC is the pore structure characteristic of many of the fuel cell components such as membrane, backing layer and catalyst layer. This paper provides a comparative study between different porous media in the PEMFC by a numerical modeling of bidirectional and steady problem of PEMFC using a single domain and a control-volume method. The model consists of non-linear, coupled partial differential equations representing the conservation of mass, momentum, species, charges and energy with electrochemical reactions valid for gas-diffusion electrodes, catalyst layers and membrane region.

This model provides results concerning the species mass fraction, potential and temperature distribution in different domain with various porosity. This model presents valuable information on the transport and heat phenomena inside the fuel cell.

Keywords PEMFC; porous media; mass; temperature

1. Introduction

Owing to their high energy efficiency, low emission, and low noise, Proton Exchange Membrane Fuel Cells (PEMFCs) are widely considered as the most promising alternative power source for automotive, portable, and stationary applications. The PEMFC may be an appropriate alternative for the internal combustion engine. The efficiency in the conversion of chemical potential energy into electrical energy; is very high compared to mechanical conversions.

Chi-Young Jung et al. [1] were conducted an investigations on effect of gas permeation coefficient in membrane, effect of membrane thickness and effect of carbon oxidation and their influences on OCP.

Seung-Gon Kim, Sang-Joon Le [2] present study, 3D structures are reconstructed by merging orthogonal-plane images. Using the 3D reconstruction, the variation of structural parameters such as the porosity in GDL is investigated under freeze-thaw cycle.

Bladimir Ramos-Alvarado et al.[3] develop an important feature of the current modeling efforts is the analysis of the main irreversibilities at different current densities showing the main energy dissipation phenomena in each cell design. Also, the hydraulic performance of the flow patterns was studied by evaluating the pressure drop and pumping power.

The purpose Daijun Yang et al.[4] study is to develop a novel binary Iridium-Cobalt/C catalyst as a suitable substitute for platinum/C applied in proton exchange membrane fuel cells (PEMFCs).

A. Eguizabal et al. [5] An innovative electrolyte membrane concept based on the synergic combination of randomly porous doped PBI membranes 80% in porosity containing H-3-methylimidazoliumbis (trifluoro methane sulfonyl) imide as intrinsic proton conductor and microporous ETS-10 coatings as diffusional barriers has been developed for High Temperature PEMFC applications.

The research Chien-Hsin Hung [6] studies an ultra-thin carbon fiber paper fabrication process for proton exchange membrane fuel cells (PEMFCs). Polyacrylonitrile (PAN) based carbon fibers 6 mm long were dispersed and formed at aerial weights of 15 and 20 g/m2 using a slurry molding machine.
The objective of the work of Djamel. Haddad [7] is to know the hydrogen, oxygen water concentration, temperature and pressure to determine the performance conditions of the fuel cell under the current density and permeability effect. A program based on the finite volume method was performed to simulate these equations system. The numerical results show that the gas distribution in the assembly membrane electrode (MEA) and the power density is affected by the nature of porous middle (permeability).

Larbi et al. [8] studies the effects of porosity and pressure on the electrolyte potential, solid potential, and oxygen mole fraction and temperature distributions have been obtained numerically.
The objective of this study is to find the effect of porosities in the transfer of potential and hydrogen in the Polymer Electrode Membrane Fuel Cell (PEMFC).

2. Theoretical Study

Figure 1 schematically shows a PEM fuel cell and its various components: two gas channels, two gas-diffusion layers, two catalyst layers and an ionometric membrane.

Figure 1: Polymer electrolyte membrane fuel cell

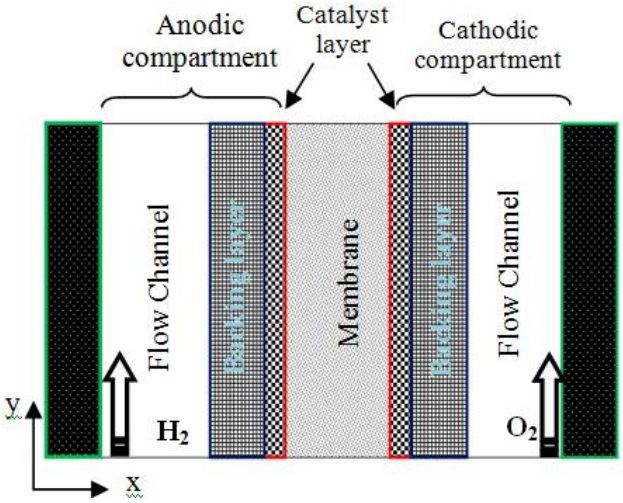

Figure 2: Model description

Governing equation:

Anode Flow Chanel: AFC

$$U\frac{\partial U}{\partial x}+V\frac{\partial U}{\partial y}=-\frac{1}{\rho}\frac{\partial P}{\partial x}+\nu\left(\frac{\partial^2 U}{\partial x^2}+\frac{\partial^2 U}{\partial y^2}\right) (1)$$

$$U\frac{\partial X_{H_2}}{\partial x}+V\frac{\partial X_{H_2}}{\partial y}=D_{H_2}^{eff}\nu\left(\frac{\partial^2 X_{H_2}}{\partial x^2}+\frac{\partial^2 X_{H_2}}{\partial y^2}\right)+S_{H_2} (2)$$

$$\rho C_p\left[U\frac{\partial T}{\partial x}+V\frac{\partial T}{\partial y}\right]=\lambda_{eff}\left[\frac{\partial^2 T}{\partial x^2}+\frac{\partial^2 T}{\partial y^2}\right]+S_T (3)$$

Anode Backing Layer: ABL

$$\frac{\partial}{\partial x}\left(\sigma_{s\,eff}\frac{\partial \phi_s}{\partial x}\right)+\frac{\partial}{\partial y}\left(\sigma_{s\,eff}\frac{\partial \phi_s}{\partial y}\right)=0 (4)$$

$$U\frac{\partial(\varepsilon^d U)}{\partial x}+V\frac{\partial(\varepsilon^d U)}{\partial y}=-\frac{\varepsilon^d}{\rho}\frac{\partial P}{\partial x}+\frac{\partial}{\partial x}\left(\nu_{eff}\frac{\partial U}{\partial x}\right)+\frac{\partial}{\partial y}\left(\nu_{eff}\frac{\partial U}{\partial y}\right)-\varepsilon^2\frac{\nu_{eff}}{k}U (5)$$

$$U\frac{\partial(\varepsilon^d V)}{\partial x}+V\frac{\partial(\varepsilon^d V)}{\partial y}=-\frac{\varepsilon^d}{\rho}\frac{\partial P}{\partial y}+\frac{\partial}{\partial x}\left(\nu_{eff}\frac{\partial V}{\partial x}\right)+\frac{\partial}{\partial y}\left(\nu_{eff}\frac{\partial V}{\partial y}\right)-\varepsilon^2\frac{\nu_{eff}}{k}V (6)$$

$$U\frac{\partial X_{H_2}}{\partial x}+V\frac{\partial X_{H_2}}{\partial y}=D_{H_2}^{eff}\nu\left(\frac{\partial^2 X_{H_2}}{\partial x^2}+\frac{\partial^2 X_{H_2}}{\partial y^2}\right)+S_{H_2}$$

Anode Catalyst Layer: ACL

$$\frac{\partial}{\partial x}\left(\sigma_{s\,eff}\frac{\partial \phi_s}{\partial x}\right)+\frac{\partial}{\partial y}\left(\sigma_{s\,eff}\frac{\partial \phi_s}{\partial y}\right)=-j_a (8)$$

$$\frac{\partial}{\partial x}\left(\sigma_{m\,eff}\frac{\partial \phi_m}{\partial x}\right)+\frac{\partial}{\partial y}\left(\sigma_{m\,eff}\frac{\partial \phi_m}{\partial y}\right)=j_a (9)$$

$$U\frac{\partial(\varepsilon^{cl} U)}{\partial x}+V\frac{\partial(\varepsilon^{cl} U)}{\partial y}=-\frac{\varepsilon^{cl}}{\rho}\frac{\partial P}{\partial x}+\frac{\partial}{\partial x}\left(\nu_{eff}\frac{\partial U}{\partial x}\right)+\frac{\partial}{\partial y}\left(\nu_{eff}\frac{\partial U}{\partial y}\right)-\frac{\nu_{eff}}{k}\varepsilon^m\varepsilon^{mc}U+\frac{k_\phi}{k_p}Z_F C_F F\left(\frac{\partial \phi_m}{\partial x}\right)$$

$$U\frac{\partial(\varepsilon^{cl} V)}{\partial x}+V\frac{\partial(\varepsilon^{cl} V)}{\partial y}=-\frac{\varepsilon^{cl}}{\rho}\frac{\partial P}{\partial y}+\frac{\partial}{\partial x}\left(\nu_{eff}\frac{\partial V}{\partial x}\right)+\frac{\partial}{\partial y}\left(\nu_{eff}\frac{\partial V}{\partial y}\right)-\frac{\nu_{eff}}{k}\varepsilon^m\varepsilon^{mc}V+\frac{k_\phi}{k_p}Z_F C_F F\left(\frac{\partial \phi_m}{\partial x}\right) (11)$$

$$U\frac{\partial X_{H_2}}{\partial x}+V\frac{\partial X_{H_2}}{\partial y}=D_{H_2}^{eff}\nu\left(\frac{\partial^2 X_{H_2}}{\partial x^2}+\frac{\partial^2 X_{H_2}}{\partial y^2}\right)+S_{H_2}$$

Membrane: MEM

$$\frac{\partial}{\partial x}(\sigma_{m\,eff}\frac{\partial \phi_m}{\partial x})+\frac{\partial}{\partial y}(\sigma_{m\,eff}\frac{\partial \phi_m}{\partial y})=0\ (13)$$

$$U\frac{\partial(\varepsilon^m U)}{\partial x}+V\frac{\partial(\varepsilon^m U)}{\partial y}=-\frac{\varepsilon^m}{\rho}\frac{\partial P}{\partial x}+\frac{\partial}{\partial x}(\nu_{eff}\frac{\partial U}{\partial x})+\frac{\partial}{\partial y}(\nu_{eff}\frac{\partial U}{\partial y})-\frac{\nu_{eff}}{k}\varepsilon^m U+\frac{k_\phi}{k_p}Z_F C_F F\left(\frac{\partial \phi_m}{\partial x}\right)\quad(14)$$

$$U\frac{\partial(\varepsilon^m V)}{\partial x}+V\frac{\partial(\varepsilon^m V)}{\partial y}=-\frac{\varepsilon^m}{\rho}\frac{\partial P}{\partial y}+\frac{\partial}{\partial x}(\nu_{eff}\frac{\partial V}{\partial x})+\frac{\partial}{\partial y}(\nu_{eff}\frac{\partial V}{\partial y})-\frac{\nu_{eff}}{k}\varepsilon^m V+\frac{k_\phi}{k_p}Z_F C_F F\left(\frac{\partial \phi_m}{\partial x}\right)(15)$$

$$U\frac{\partial X_{H_2O}}{\partial x}+V\frac{\partial X_{H_2O}}{\partial y}=D^{eff}_{H_2O}\nu(\frac{\partial^2 X_{H_2O}}{\partial x^2}+\frac{\partial^2 X_{H_2O}}{\partial y^2})+S_{H_2O}\ (16)$$

Cathode Catalyst Layer: CCL

$$\frac{\partial}{\partial x}(\sigma_{s\,eff}\frac{\partial \phi_s}{\partial x})+\frac{\partial}{\partial y}(\sigma_{s\,eff}\frac{\partial \phi_s}{\partial y})=j_c\ (17)$$

$$\frac{\partial}{\partial x}(\sigma_{m\,eff}\frac{\partial \phi_m}{\partial x})+\frac{\partial}{\partial y}(\sigma_{m\,eff}\frac{\partial \phi_m}{\partial y})=-j_c\ (18)$$

$$U\frac{\partial(\varepsilon^{cl} U)}{\partial x}+V\frac{\partial(\varepsilon^{cl} U)}{\partial y}=-\frac{\varepsilon^{cl}}{\rho}\frac{\partial P}{\partial x}+\frac{\partial}{\partial x}(\nu_{eff}\frac{\partial U}{\partial x})+\frac{\partial}{\partial y}(\nu_{eff}\frac{\partial U}{\partial y})-\frac{\nu_{eff}}{k}\varepsilon^m\varepsilon^{mc} U+\frac{k_\phi}{k_p}Z_F C_F F\left(\frac{\partial \phi_m}{\partial x}\right)(19)$$

$$U\frac{\partial(\varepsilon^{cl} V)}{\partial x}+V\frac{\partial(\varepsilon^{cl} V)}{\partial y}=-\frac{\varepsilon^{cl}}{\rho}\frac{\partial P}{\partial y}+\frac{\partial}{\partial x}(\nu_{eff}\frac{\partial V}{\partial x})+\frac{\partial}{\partial y}(\nu_{eff}\frac{\partial V}{\partial y})-\frac{\nu_{eff}}{k}\varepsilon^m\varepsilon^{mc} V+\frac{k_\phi}{k_p}Z_F C_F F\left(\frac{\partial \phi_m}{\partial x}\right)(20)$$

$$U\frac{\partial X_{O_2}}{\partial x}+V\frac{\partial X_{O_2}}{\partial y}=D^{eff}_{O_2}\nu(\frac{\partial^2 X_{O_2}}{\partial x^2}+\frac{\partial^2 X_{O_2}}{\partial y^2})+S_{O_2}(21)$$

Cathode Backing Layer:CBL

$$\frac{\partial}{\partial x}(\sigma_{s\,eff}\frac{\partial \phi_s}{\partial x})+\frac{\partial}{\partial y}(\sigma_{s\,eff}\frac{\partial \phi_s}{\partial y})=0\ (22)$$

$$U\frac{\partial(\varepsilon^d U)}{\partial x}+V\frac{\partial(\varepsilon^d U)}{\partial y}=-\frac{\varepsilon^d}{\rho}\frac{\partial P}{\partial x}+\frac{\partial}{\partial x}(\nu_{eff}\frac{\partial U}{\partial x})+\frac{\partial}{\partial y}(\nu_{eff}\frac{\partial U}{\partial y})-\varepsilon^2\frac{\nu_{eff}}{k}U\ (23)$$

$$U\frac{\partial(\varepsilon^d V)}{\partial x}+V\frac{\partial(\varepsilon^d V)}{\partial y}=-\frac{\varepsilon^d}{\rho}\frac{\partial P}{\partial y}+\frac{\partial}{\partial x}(\nu_{eff}\frac{\partial V}{\partial x})+\frac{\partial}{\partial y}(\nu_{eff}\frac{\partial V}{\partial y})-\varepsilon^2\frac{\nu_{eff}}{k}V\ (24)$$

$$U\frac{\partial X_{O_2}}{\partial x}+V\frac{\partial X_{O_2}}{\partial y}=D_{O_2}^{eff}v(\frac{\partial^2 X_{O_2}}{\partial x^2}+\frac{\partial^2 X_{O_2}}{\partial y^2})+S_{O_2}\ (25)$$

Cathode Flow Chanel: CFC

$$U\frac{\partial U}{\partial x}+V\frac{\partial U}{\partial y}=-\frac{1}{\rho}\frac{\partial P}{\partial x}+v(\frac{\partial^2 U}{\partial x^2}+\frac{\partial^2 U}{\partial y^2})\ (26)$$

$$U\frac{\partial X_{O_2}}{\partial x}+V\frac{\partial X_{O_2}}{\partial y}=D_{O_2}^{eff}v(\frac{\partial^2 X_{O_2}}{\partial x^2}+\frac{\partial^2 X_{O_2}}{\partial y^2})+S_{O_2}$$

$$\rho C_p[U\frac{\partial T}{\partial x}+V\frac{\partial T}{\partial y}]=\lambda_{eff}[\frac{\partial^2 T}{\partial x^2}+\frac{\partial^2 T}{\partial y^2}]+S_T\ (28)$$

3. Sources Terms

Hydrogen

$$\begin{cases}S_{H_2}=-\dfrac{j_a}{2FC_{tot}^a} & \text{in the ACL}\\ S_{H_2}=0 & \text{outside}\end{cases}$$

Oxygen

$$\begin{cases}S_{O_2}=\dfrac{j_c}{4FC_{tot}^c} & \text{in CCL}\\ S_{O_2}=0 & \text{outside}\end{cases}$$

Water

$$\begin{cases}S_{H_2O}=-\dfrac{j_c}{2FC_{tot}^c}\\ S_{H_2O}=0 & \text{outside}\end{cases}$$

Temperature

$$S_T=\begin{cases}S_T=i\eta+\dfrac{i^2}{\sigma_m} & \text{ACL, CCL}\\ S_T=\dfrac{i^2}{\sigma_m} & \text{MEM}\\ S_T=0 & \text{outside}\end{cases}$$

4. Results and Discussions

The membrane porosity affects numerous transport parameters that are important for the fuel cell operation. The figures 2,3 and 4 show that the membrane potential decreases from the anode to the cathode. This decrease is due to the weak over potential in the anode catalyst layer and an important over potential in the cathode catalyst layer. This indicates that the hydrogen oxidation kinetics on the anode is much faster than the cathode reaction. The most important loss mechanism is the activation over potential at the cathode side. The membrane potential distribution depends on the membrane porosity. This difference is clearly shown in the membrane region.

The activation overpotential decreases with increasing the membrane porosity. This is because the exchange current density of the oxygen reduction reaction increases with decreasing of the membrane porosity due to the enhanced reaction kinetics.

The potential in the anode is little than the potential in the cathode. This is due to the fact that the cathode over-potential is more important than the anode over-potential

The local solid phase potential in the cathode depends on the catalyst layer porosities. The local potential increases with increasing the porosity. The variation in the local solid phase potential can be attributed to the solid phase conductivity, which is a function of porosity.

The effect of backing layer porosity has been studied on the fuel cell Performance in figure 5, 6 and 7.The figures shows when we increase the porosity from 30% to 50%, the cathodic potential deceases. The figures 8 and 9 show the hydrogen distribution for two different backing layer porosities, when we increase the porosity the diffusion is easier for H2. The result shows that the pore assists the transport of hydrogen through the backing layer. Therefore, when the porosities are greater, the diffusion of species is easier in the gas diffusion layer. Therefore there is a proportionality between the porosity and the mole fraction of hydrogen. The porosity of the gas diffusion layer has two comparing effects on the fuel cell performance; as the porous region provides the space for the reactants to diffuse towards the catalyst region, an increase in the porosity means that the onset of mass transport limitations occurs at higher current densities, i.e. it leads to higher limiting currents.

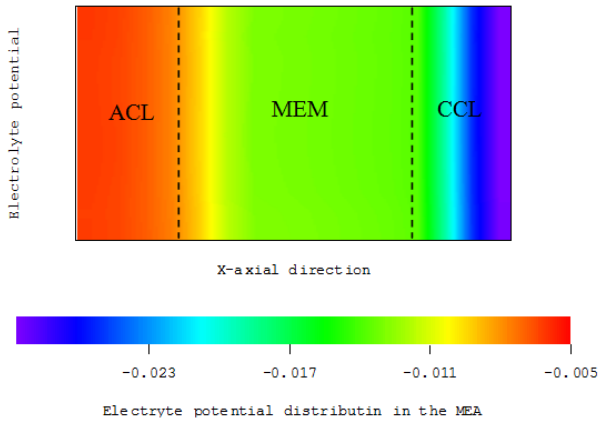

Figure 3: Electrolyte potential for membrane porosity =20%

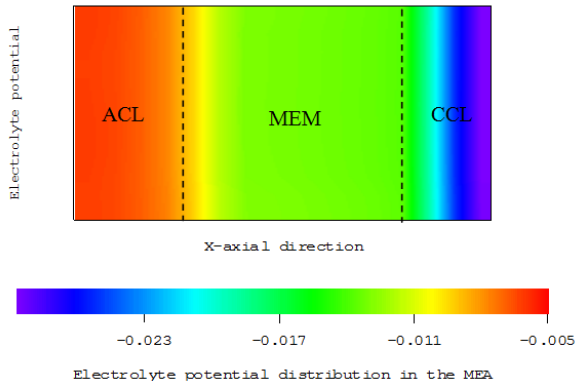

Figure 4: Electrolyte potential for membrane porosity =28%

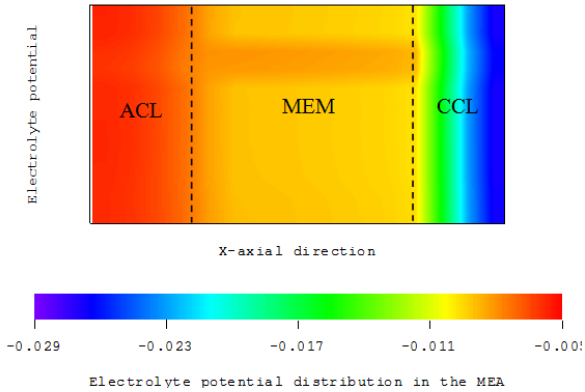

Figure 5: Electrolyte potential for membrane porosity =40%

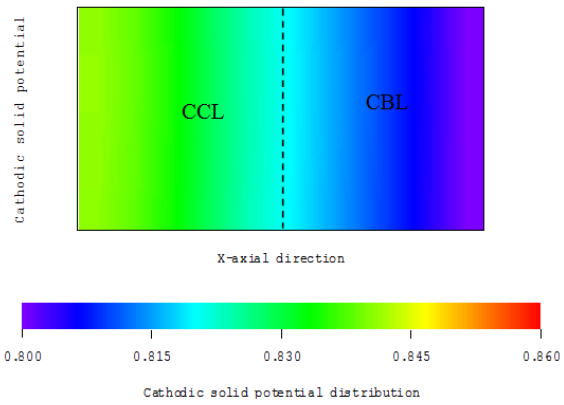

Figure 6: Cathodic solid potential for BL porosity 30%

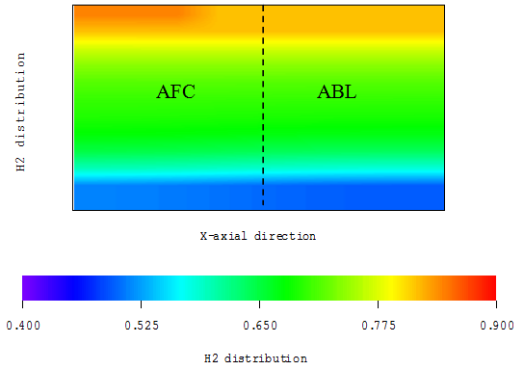

Figure 9: Hydrogen distribution for BL porosity= 30%

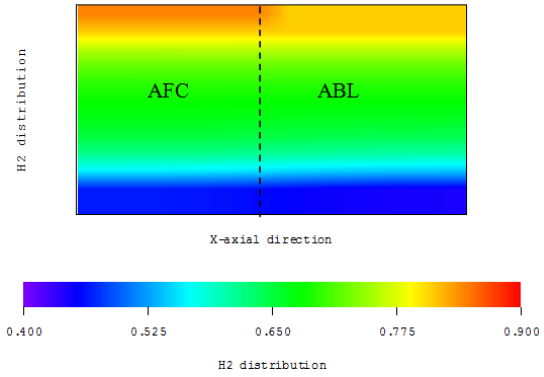

Figure 10: Hydrogen distribution for BL porosity= 40%

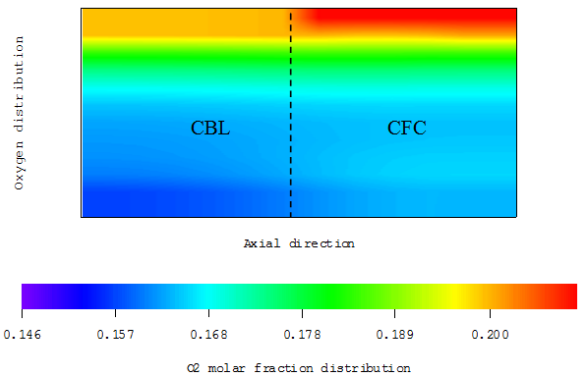

Figure 11: Oxygen distribution for cathodic pressure = 3bar with same BL porosity

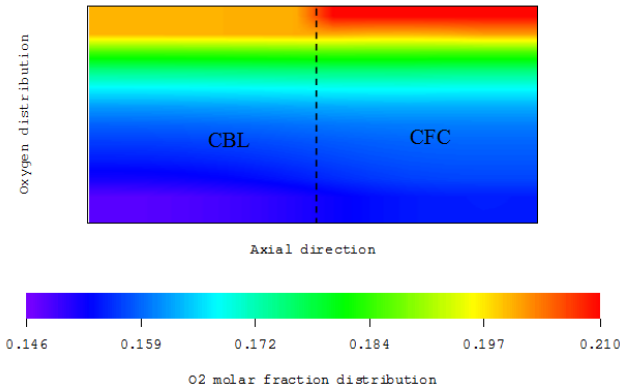

Figure 12: Oxygen distribution for cathodic pressure = 4bar with same BL porosity

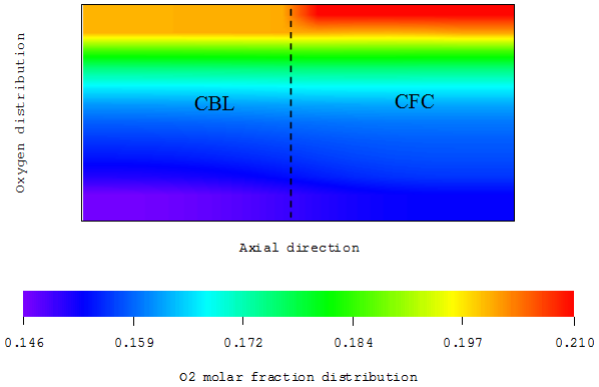

Figure 13: Oxygen distribution for cathodic pressure = 5bar with same BL porosity

The pressure is an important parameter for the operation of the PEMFC.

Figures 10, 11, and 12 show the distribution of the oxygen concentration value for different cathode inlet pressure. The results show that for higher inlet pressure (P = 5 bar) the oxygen molar fraction will be increased. As the pressure increases with the oxygen concentration in the cathode side, the overall performance of the cell increases as the over potential concentration effects becomes smaller. This is due to the fact that the local production of current is linearly dependent on the local concentration as given by the Butler-Volmer equation. The performance of the PEM fuel cell can be significantly improved by increasing inlet pressure, but in practice, this increase has a limit because the membrane cannot sustain a large pressure difference between the anode and the cathode can result in internal leakages of the oxidant. In addition to the high-pressure applications need a better seal.

5. Conclusion

The performance of the PEM fuel cell is simulated with various operating conditions. We can deduce that the solid and electrolyte potential depend on the porosities of membrane and backing layer.

The hydrogen concentration decreases from inlet to outlet and depends on the backing layer porosity; also the oxygen concentration depends on cathodic inlet pressure.

Porous materials play a key role in the development of fuel cell technology. The function of these porous materials includes the transport of gases to and from the active sites and pressure can be a solution to optimize the performance of the PEM-FC.

References

[1]. Chi-Young Jung, Wha-Jung Kim , Sung-Chul Yi , “Computational analysis of mixed potential effect in proton exchange membrane fuel cells,” International journal of hydrogen energy,37 (2012) 7654-7668 .

[2]. Seung-Gon Kim, Sang-Joon LeeJ. "Tomographic analysis of porosity variation in gas diffusion layer under freeze-thaw cycles" International journal of hydrogen energy,37 (2012) 566-574.

[3]. Bladimir Ramos-Alvarado, Abel Hernandez-Guerrero, Daniel Juarez Robles, Peiwen Li," Numerical investigation of the performance of symmetric flow distributors as flow channels for PEM fuel cells, International journal of hydrogen energy,37 (2012) 436-448.

[4]. Daijun Yang, Bing Li, Hao Zhang, Jianxin Ma, Kinetics and electrocatalytic activity of IrCo/C catalysts for oxygen reduction reaction in PEMFC, International journal of hydrogen energy,37 (2012) 2447-2454

[5]. A. Eguiza, J.Lemus, V. Roda, M. Urbiztondo, F. Barreras, M.P. Pina "Nanostructured electrolyte membranes based on zeotypes, protic ionic liquids and porous PBI membranes: Preparation, characterization and MEA testing" International journal of hydrogen energy,37 (2012) 7221-7234

[6]. Chien-Hsin Hung, Cheng-Hao Chiu, Shuo-Ping Wang, I-Long Chiang ,Hsiharng Yang. " Ultra thin gas diffusion layer development for PEMFC" International journal of hydrogen energy,37 (2012) 12805-12812

[7]. Haddad D, et al., Transport phenomena effect on the performance of proton exchangemembrane fuel cell (PEMFC), International Journal of Hydrogen Energy (2012), http://dx.doi.org/10.1016/j.ijhydene.2012.11.011

[8]. Badreddine Larbi, Wael Alimi, Ridha Chouikh, Amenallah Guizani Effect of porosity and pressure on the PEM fuel cell performance" International journal of hydrogen energy, 38 (2013) 8542-8549